THE EUROPEAN PHYSICAL JOURNAL C

CrossMark

Regular Article - Theoretical Physics

Warm $\frac{\lambda}{4}\phi^4$ inflationary universe model in light of Planck 2015 results

Grigorios Panotopoulos[a], **Nelson Videla**[b]

Departamento de Física, FCFM, Universidad de Chile, Blanco Encalada 2008, Santiago, Chile

Abstract   In the present work we show that warm chaotic inflation characterized by a simple $\frac{\lambda}{4}\phi^4$ self-interaction potential for the inflaton, excluded by current data in standard cold inflation, and by an inflaton decay rate proportional to the temperature, is in agreement with the latest Planck data. The parameters of the model are constrained, and our results show that the model predicts a negligible tensor-to-scalar ratio in the strong dissipative regime, while in the weak dissipative regime the tensor-to-scalar ratio can be large enough to be observed.

1 Introduction

The inflationary universe has become one of the central paradigms in modern cosmology. This is due to the fact that many long-standing problems of the Big Bang model, such as the horizon, flatness, homogeneity, and monopole problems, find a natural explanation in the framework of the inflationary universe [1–6]. However, the essential feature of inflation is that it generates a mechanism to explain the Large-Scale Structure (LSS) of the universe [7–11] and provides a causal interpretation of the origin of the anisotropies observed in the Cosmic Microwave Background (CMB) radiation [12–17], since primordial density perturbations may be produced from quantum fluctuations during the inflationary era.

The original "old inflation" scenario assumed the inflaton was trapped in a metastable false vacuum and had to exit to the true vacuum via a first-order transition [1,2]. However, the exit could occur neither gracefully nor completely. The revised version of inflation was proposed by Linde [3,4], and Albrecht and Steinhardt [5] in 1982 referred as "new inflation". However, these scenarios suffer from theoretical problems about the duration of inflation and initial conditions. In

1983, Linde considered the case that the initial conditions for scalar field driving inflation may be chaotic, which is called "chaotic inflation" [6]. This inflation model can solve the remaining problems, where the potential was chosen to be quadratic or quartic form, i.e. $\frac{m^2}{2}\phi^2$ or $\frac{\lambda}{4}\phi^4$, terms that are always present in the scalar potential of the Higgs sector in all renormalizable gauge field theories [18] in which the gauge symmetry is spontaneously broken via the Englert–Brout–Higgs mechanism [19,20]. Such models are interesting for their simplicity, and has become one of the most favored, because they predict a significant amount of tensor perturbations due to the inflaton field gets across the trans-Planckian distance during inflation [21]. After that, many kinds of inflationary scenarios have been proposed, related to supersymmetry (SUSY) theory, brane world, string theory, etc. (for a review, see [22–25]).

On the other hand, with respect to the dynamical mechanisms of inflation, the warm inflation scenario, as opposed to the standard cold inflation, has the attractive feature that it avoids the reheating period at the end of the accelerated expansion [26,27]. During the evolution of warm inflation dissipative effects are important, and radiation production takes place at the same time as the expansion of the universe. The dissipative effects arise from a friction term which accounts for the processes of the scalar field dissipating into a thermal bath. In further relation to these dissipative effects, the dissipative coefficient Γ is a fundamental quantity, which has been computed from first principles in the context of supersymmetry. In particular, in Ref. [28], a supersymmetric model containing three superfields Φ, X, and Y has been studied, with a superpotential $W = \frac{g}{\sqrt{2}}\Phi X^2 - \frac{h}{\sqrt{2}}XY^2$, where the scalar components of the superfields are ϕ, χ, and y, respectively. For a scalar field with multiplets of heavy and light fields, and different decay mechanisms, it is possible to obtain several expressions for the dissipative coefficient Γ; see e.g., [28–34].

[a] e-mail: gpanotop@ing.uchile.cl

[b] e-mails: nelson.videlamenares@gmail.com;
            nelson.videla@ing.uchile.cl

Springer

Following Refs. [31,32], a general parametrization of the dissipative coefficient $\Gamma(T, \phi)$ can be written as

$$\Gamma(T, \phi) = a \frac{T^m}{\phi^{m-1}}, \tag{1}$$

where the parameter a is related with the dissipative microscopic dynamics and the exponent m is an integer. This expression for the dissipative coefficient includes different cases studied in the literature, depending of the values of m (see Refs. [31,32]). Specifically, for the value $m = 3$, i.e., $\Gamma \propto T^3/\phi^2$, the parameter a corresponds to $0.02h^2\mathcal{N}_Y$, where a generic supersymmetric model with chiral superfields Φ, X, and Y_i, $i = 1, \ldots, \mathcal{N}_Y$ has been considered. This case corresponds to a low temperature regime, when the mass of the catalyst field m_χ is larger than the temperature T [33,34]. On the other hand, $m = 1$, i.e., $\Gamma \propto T$ corresponds to a high temperature regime, where the thermal corrections to the catalyst field mass start to be important, where $a = 0.97g^2/h^2$ [28]. For $m = 0$, the dissipative coefficient represents an exponentially decaying propagator in the high temperature regime. Finally, for $m = -1$, i.e., $\Gamma \propto \phi^2/T$, we have agreement with the non-SUSY case [29,35]. Additionally, thermal fluctuations during the inflationary scenario may play a fundamental role in producing the primordial fluctuations [36,37]. During the warm inflationary scenario the density perturbations arise from thermal fluctuations of the inflaton and dominate over the quantum ones. In this form, an essential condition for warm inflation to occur is the existence of a radiation component with temperature $T > H$, since the thermal and quantum fluctuations are proportional to T and H, respectively [26,27,36,37]. When the universe heats up and becomes radiation dominated, inflation ends and the universe smoothly enters the radiation Big Bang phase [26,27]. For a comprehensive review of warm inflation, see Refs. [38,39].

Upon comparison to the current cosmological and astronomical observations, specially those related with the CMB temperature anisotropies, it is possible to constrain the inflationary models. In particular, the constraints in the $n_s - r$ plane give us the predictions of a number of representative inflationary potentials. Recently, the Planck collaboration has published new data of enhanced precision of the CMB anisotropies [40]. Here, the Planck full mission data has improved the upper bound on the tensor-to-scalar ratio $r_{0.002} < 0.11$ (95 % CL) which is similar to obtained from [17], in which $r < 0.12$ (95 % CL). In particular, the $\frac{\lambda}{4}\phi^4$ model, which predicts a large value of the tensor-to-scalar ratio r, lies well outside of the joint 99.7 % CL region in the r–n_s plane, so it is ruled out by the data. This result confirms previous findings by, e.g., Hinshaw et al. [15] in which this model is well outside the 95 % CL for the WMAP 9-year data and is further excluded by CMB data at smaller scales.

In this way, the goal of the present work is to study the possibility that the $\frac{\lambda}{4}\phi^4$ model can be rescued in the warm inflation scenario and be able to agree with the latest observational data. In order to achieve this, we consider an inflaton decay rate Γ proportional to the temperature, which has been computed in the context of a high temperature supersymmetric model [28]. We stress that in previous works (see Refs. [33,34]) the authors have also studied the quartic potential in the framework of warm inflation. However, our work is different in two ways. First, contrary to the standard cold inflation where the dynamics is determined only by the inflaton potential, in warm inflation also the dissipative coefficient plays an important role, and here we have considered an expression for it not studied in the previous works. Furthermore, in none of these papers the authors used the contour plots in the r–n_s plane to constrain the parameters of the model they studied. On the contrary, in our work here we have used the latest data from Planck, not available at that time, to put bounds on the parameters of the model we have considered.

The outline of the paper is as follows: The next section presents a short review of the basics of warm inflation scenario. In Sect. 3 we study the dynamics of warm inflation for our quartic potential, in the weak and strong dissipative regimes; specifically, we obtain analytical expressions for the slow-roll parameters and the dissipative coefficient. Immediately, we compute the cosmological perturbations in both dissipative regimes, obtaining expressions for the inflationary observables such as the scalar power spectrum, the scalar spectral index, and the tensor-to-scalar ratio. Finally, Sect. 4 summarizes our results and exhibits our conclusions. We choose units so that $c = \hbar = 1$.

2 Basics of warm inflation scenario

2.1 Background evolution

We start by considering a spatially flat Friedmann–Robertson–Walker (FRW) universe containing a self-interacting inflaton scalar field ϕ with energy density and pressure given by $\rho_\phi = \dot{\phi}^2/2 + V(\phi)$ and $P_\phi = \dot{\phi}^2/2 - V(\phi)$, respectively, and a radiation field with energy density ρ_γ. The corresponding Friedmann equation reads

$$H^2 = \frac{1}{3M_p^2}(\rho_\phi + \rho_\gamma), \tag{2}$$

where $M_p = \frac{1}{\sqrt{8\pi G}}$ is the reduced Planck mass.

The dynamics of ρ_ϕ and ρ_γ is described by the equations [26,27]

$$\dot{\rho}_\phi + 3H(\rho_\phi + P_\phi) = -\Gamma\dot{\phi}^2, \tag{3}$$

and

$$\dot{\rho}_\gamma + 4H\rho_\gamma = \Gamma\dot{\phi}^2, \tag{4}$$

where the dissipative coefficient $\Gamma > 0$ produces the decay of the scalar field into radiation. Recall that this decay rate can be assumed to be a function of the temperature of the thermal bath $\Gamma(T)$, or a function of the scalar field $\Gamma(\phi)$, or a function of $\Gamma(T, \phi)$ or simply a constant [26,27].

During warm inflation, the energy density related to the scalar field predominates over the energy density of the radiation field, i.e., $\rho_\phi \gg \rho_\gamma$ [26,27,36,41–43], but even if small when compared to the inflaton energy density it can be larger than the expansion rate with $\rho_\gamma^{1/4} > H$. Assuming thermalization, this translates roughly into $T > H$, which is the condition for warm inflation to occur.

When H, ϕ, and Γ are slowly varying, which is a good approximation during inflation, the production of radiation becomes quasi-stable, i.e., $\dot{\rho}_\gamma \ll 4H\rho_\gamma$ and $\dot{\rho}_\gamma \ll \Gamma\dot{\phi}^2$; see Refs. [26,27,36,41–43]. Then the equations of motion reduce to

$$3H(1+R)\dot{\phi} \simeq -V_{,\phi}, \tag{5}$$

where, ϕ denotes differentiation with respect to inflaton, and

$$4H\rho_\gamma \simeq \Gamma\dot{\phi}^2, \tag{6}$$

where R is the dissipative ratio defined as

$$R \equiv \frac{\Gamma}{3H}. \tag{7}$$

In warm inflation, we can distinguish between two possible scenarios, namely the weak and strong dissipative regimes, defined as $R \ll 1$ and $R \gg 1$, respectively. In the weak dissipative regime, the Hubble damping is still the dominant term, however, in the strong dissipative regime, the dissipative coefficient Γ controls the damped evolution of the inflaton field.

If we consider thermalization, then the energy density of the radiation field could be written as $\rho_\gamma = C_\gamma T^4$, where the constant $C_\gamma = \pi^2 g_*/30$. Here, g_* represents the number of relativistic degrees of freedom. In the Minimal Supersymmetric Standard Model (MSSM), $g = 228.75$ and $C_\gamma \simeq 70$ [36]. Combining Eqs. (5) and (6) with $\rho_\gamma \propto T^4$, the temperature of the thermal bath becomes

$$T = \left[\frac{\Gamma V_{,\phi}^2}{36C_\gamma H^3(1+R)^2}\right]^{1/4}. \tag{8}$$

On the other hand, the consistency conditions for the approximations to hold imply that a set of slow-roll conditions must be satisfied for a prolonged period of inflation to take place. For warm inflation, the slow-roll parameters are [28,36]

$$\epsilon = \frac{M_p^2}{2}\left(\frac{V_{,\phi}}{V}\right)^2, \quad \eta = M_p^2\left(\frac{V_{,\phi\phi}}{V}\right),$$
$$\beta = M_p^2\left(\frac{\Gamma_{,\phi}V_{,\phi}}{\Gamma V}\right), \quad \sigma = M_p^2\left(\frac{V_{,\phi}}{\phi V}\right). \tag{9}$$

The slow-roll conditions for warm inflation can be expressed as [28,36]

$$\epsilon \ll 1+R, \quad \eta \ll 1+R, \quad \beta \ll 1+R, \quad \sigma \ll 1+R \tag{10}$$

When one these conditions is not longer satisfied, either the motion of the inflaton is no longer overdamped and slow-roll ends, or the radiation becomes comparable to the inflaton energy density. In this way, inflation ends when one of these parameters become the order of $1 + R$.

From first principles in quantum field theory, the dissipative coefficient Γ has been computed. As we have seen in the introduction, the parametrization given by Eq. (1) includes different cases, depending of the values of m. Concretely, for $m = 3$, for which $\Gamma = aT^3\phi^{-2}$, the parameter a agrees with $a = 0.02 h^2 \mathcal{N}_Y$, where a generic supersymmetric model with chiral superfields Φ, X, and Y_i, $i = 1, ..., \mathcal{N}_Y$ has been considered. In particular, this inflation ratio decay has been studied extensively in the literature [33,34,44–46], including the quartic potential [38,39]. For the special case $m = 1$, the dissipative coefficient $\Gamma \propto T$ is related with the high temperature supersymmetry (SUSY) case [28]. Finally, for the cases $m = 0$ and $m = -1$, Γ represents an exponentially decaying propagator in the high temperature SUSY model and the non-SUSY case, respectively [29,35].

2.2 Perturbations

In the warm inflation scenario, a thermalized radiation component is present with $T > H$, then the inflaton fluctuations $\delta\phi$ are predominantly thermal instead quantum. In this way, following [36–39], the amplitude of the power spectrum of the curvature perturbation is given by

$$\mathcal{P}_\mathcal{R}^{1/2} \simeq \left(\frac{H}{2\pi}\right)\left(\frac{3H^2}{V_\phi}\right)(1+R)^{5/4}\left(\frac{T}{H}\right)^{1/2}, \tag{11}$$

where the normalization has been chosen in order to recover the standard cold inflation result when $R \to 0$ and $T \simeq H$.

On the other hand, the scalar spectral index n_s is given by [36]

$$n_s = 1 + \frac{d\mathcal{P}_\mathcal{R}}{d\ln k} \simeq 1 + \frac{1}{1+R}[-(2-5A_R)\epsilon - 3A_R\eta + (2+4A_R)\sigma], \tag{12}$$

where $A_R = \frac{R}{1+7R}$.

Regarding tensor perturbations, these do not couple to the thermal background, so gravitational waves are only generated by quantum fluctuations, as in standard inflation [47]. However, the tensor-to-scalar ratio r is modified with respect to standard cold inflation, yielding [38,39]

$$r \simeq \left(\frac{H}{T}\right) \frac{16\epsilon}{(1+R)^{5/2}}. \tag{13}$$

We can see that warm inflation predicts a tensor-to-scalar ratio suppressed by a factor $(T/H)(1+R)^{5/2} > 1$ compared with standard cold inflation.

When a specific form of the scalar potential and the dissipative coefficient Γ are considered, it is possible to study the background evolution under the slow-roll regime and the primordial perturbations in order to test the viability of warm inflation. In the following we will study how an inflaton decay rate proportional to the temperature, corresponding to the case $m = 1$, influences the inflationary dynamics for the quartic potential. We will restrict ourselves to the weak and strong dissipation regimes.

3 Dynamics of warm $\frac{\lambda}{4}\phi^4$ inflation

Although inflation is widely accepted as the standard paradigm for the early universe, it is not a theory yet as we do not know how to answer the question that naturally arises, "what is the inflaton and what is its potential?". After the recent discovery of the Higgs boson at CERN [48,49], which showed that elementary scalars exist in nature, the most natural and simplest thing to assume is that inflation is driven by the Higgs boson (in the standard model or in some extension of it). Unfortunately it is well known that the quartic potential, which is the simplest Higgs potential provided by particle physics in renormalizable theories, has been excluded by current data [50] since it predicts too many gravity waves. Although the presence of a non-minimal coupling can make the quartic potential viable [51,52], warm inflation provides another solution that is simpler and at the same time, as we have already mentioned, avoids the discussion as regards reheating. If we look at the expressions for the observables in the framework of warm inflation, we see that the key ingredient that can in principle reduce the tensor-to-scalar ratio and bring the predictions of the model inside the region allowed by observational data, is the suppression factors (T/H) and $R^{5/2}$. This is exactly what happens indeed as we will show in the discussion to follow.

Warm inflation with a quartic potential for the inflaton has also been studied in [32,53,54]. However, there are some differences, as in these works the authors have used another expression for the dissipative coefficient; they have not derived the allowed range for the parameters of the model

they studied, and finally in our work we have used the most recent data available today.

3.1 The weak dissipative regime

Considering that our model evolves in agreement with the weak dissipative regime, where $R \ll 1$, and that under the slow-roll approximation the Friedmann and the Klein–Gordon equations take the standard form, the temperature of the radiation field, assuming an inflaton potential of the form $V(\phi) = (1/4)\lambda\phi^4$ and an inflaton decay rate $\Gamma = aT$, becomes

$$T \simeq \left(\frac{aV_{,\phi}^2}{36C_\gamma H^3}\right)^{1/3}, \tag{14}$$

and the Hubble parameter is given by

$$H \simeq \left(\frac{V}{3M_p^2}\right)^{1/2}. \tag{15}$$

In this way, for the weak regime, the slow-roll parameters become

$$\epsilon = \frac{8M_p^2}{\phi^2}, \quad \eta = \frac{12M_p^2}{\phi^2}, \quad \beta = 0, \quad \sigma = \frac{4M_p^2}{\phi^2}. \tag{16}$$

It is easy to see that the end of inflation is determined by the condition $\eta = 1$, where the scalar field takes the value $\phi_{\rm end} = 2\sqrt{3}M_p$.

On the other hand, the number of e-folds is given by the standard formula

$$N = \int_{t_*}^{t_{\rm end}} H \, {\rm d}t \simeq \frac{1}{M_p^2} \int_{\phi_{\rm end}}^{\phi_*} \frac{V}{V_\phi} \, {\rm d}\phi \simeq \frac{1}{4}\left(\frac{\phi_*}{M_p}\right)^2, \tag{17}$$

where we have assumed that $\phi_* \gg \phi_{\rm end}$.

In the following, we will study the scalar and tensor perturbations. In the weak dissipative regime, the amplitude of the power spectrum (11) becomes

$$\mathcal{P}_\mathcal{R}^{1/2} \simeq \left(\frac{H}{2\pi}\right)\left(\frac{3H^2}{V_{,\phi}}\right)\left(\frac{T}{H}\right)^{1/2}. \tag{18}$$

By using Eqs. (14), (15), and (17), it may we written in terms in the number of e-folds as

$$\mathcal{P}_\mathcal{R}^{1/2} \simeq \left(\frac{\lambda\sqrt{a}N^3}{6\sqrt{70}\pi^3}\right)^{1/3}. \tag{19}$$

The power spectrum constraint $P_R^{1/2} \sim 10^{-5}$ [17,40] determines the dimensionless coupling λ in terms of a and N,

while the scalar spectral index (12) turns out to be

$$n_s \simeq 1 - 2\epsilon + 2\sigma, \tag{20}$$

which may be expressed in terms of the number of the e-folds, obtaining

$$n_s = 1 - \frac{1}{N}, \tag{21}$$

while the tensor-to-scalar ratio (13) becomes

$$r \simeq \left(\frac{H}{T}\right) 16\epsilon, \tag{22}$$

so eventually we can obtain r as a function of n_s. Using Eqs. (19), (21), and (22), the relation $r(n_s)$ is given by

$$r = \frac{4\sqrt{14}}{625\sqrt{5}\, a^{1/2}} (1 - n_s). \tag{23}$$

In Fig. 1, the relation $r(n_s)$ is shown for several values of a. In the same plot we also show the curve for standard inflation ($a = 0$) as well as the contours allowed by the Planck latest data. When a decreases the curve is shifted upwards and finally lies outside the allowed contours. This induces a lower bound on a. On the other hand, when a increases the curve is shifted downwards, but R also increases and eventually the condition for being in the weak dissipative regime is violated. This induces an upper bound on a, which is found to be
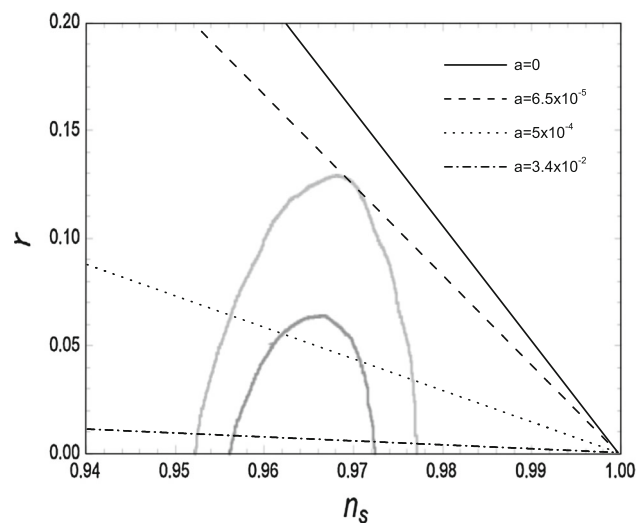

Fig. 1 Plot of the tensor-to-scalar ratio r versus the scalar spectral index n_s in the weak dissipative regime, for the quartic potential and an inflaton ratio decay $\Gamma = aT$. Here, we have considered the two-dimensional marginalized joint confidence contours for (n_s, r), at the 68 and 95 % CL, from the latest Planck data [40]. In this plot we have used four different values of the parameter a, where the value $a = 0$ corresponds to standard cold inflation

$6.5 \times 10^{-5} < a < 3.4 \times 10^{-2}$. This implies that Eq. (19), evaluated when the cosmological scales cross the Hubble horizon during inflation at 60 e-folds, gives us the constraint on λ determined by $10^{-15} < \lambda < 10^{-13}$. It is interesting to note that this result is in agreement with the value obtained for λ in the standard cold inflation using the COBE normalization [55], given by $\lambda \sim 10^{-14}$.

3.2 The strong dissipative regime

Considering that our model evolves in agreement with the strong dissipative regime, where $R \gg 1$, under the slow-roll approximation, the temperature of the radiation field becomes

$$T \simeq \left(\frac{V_{,\phi}^2}{4C_\gamma\, aH}\right)^{1/5}, \tag{24}$$

and the Hubble parameter is given by Eq. (15). In this way, for the strong regime, the slow-roll parameters become

$$\epsilon = \frac{8M_p^2}{\phi^2}, \quad \eta = \frac{12M_p^2}{\phi^2}, \quad \beta \frac{15M_p^2}{5\phi^2}, \quad \sigma = \frac{4M_p^2}{\phi^2}. \tag{25}$$

For the strong regime, inflation ends when one of these slow-roll parameters becomes the order of R. In this case, the end of inflation is determined by the condition $\eta = R$, where the inflaton takes the value $\phi_{\text{end}} = \frac{(6^7 35)^{1/4}}{a} \lambda^{1/4} M_p$.

On the other hand, the number of e-folds is given by

$$\begin{aligned} N &= \int_{t_*}^{t_{\text{end}}} H\, dt \simeq \frac{1}{M_p^2} \int_{\phi_{\text{end}}}^{\phi_*} \frac{V}{V_\phi} R\, d\phi \\ &\simeq \frac{1}{8} \left(\frac{a\, 5^4}{7\lambda 6^2}\right)^{1/5} \left(\frac{\phi_*}{M_p}\right)^{4/5}, \end{aligned} \tag{26}$$

where we have assumed that $\phi_* \gg \phi_{\text{end}}$.

Now, the amplitude of the power spectrum (11) becomes

$$\mathcal{P}_{\mathcal{R}}^{1/2} \simeq \left(\frac{H}{2\pi}\right) \left(\frac{3H^2}{V_\phi}\right) \left(\frac{T}{H}\right)^{1/2} R^{5/4}, \tag{27}$$

Similarly to the weak regime, the amplitude of the power spectrum may we written in terms of the number of e-folds. Using Eqs. (15), (24), and (26), we have

$$\mathcal{P}_{\mathcal{R}}^{1/2} \simeq \left[\frac{4N^3\lambda}{125\pi^{8/3}} \left(\frac{2}{315}\right)^{1/3}\right]^{3/8}. \tag{28}$$

In this case, the power spectrum does not depend on a and then the constraint $P_R^{1/2} \sim 10^{-5}$ [17,40] determines the inflaton self-interaction coupling λ.

For this regime, the scalar spectral index (12) turns out to be

$$n_s \simeq 1 + \frac{1}{7R}(-3\eta + 18\sigma - 9\epsilon), \tag{29}$$

which expressed in terms of the number of the e-folds yields

$$n_s = 1 - \frac{45}{28N}. \tag{30}$$

Finally, for the tensor-to-scalar ratio (13) we have

$$r \simeq \left(\frac{H}{T}\right)\frac{16\,\epsilon}{R^{5/2}}, \tag{31}$$

which may be expressed as a function of n_s. Using Eqs. (28), (30), and (31), the relation $r(n_s)$ is given by

$$r \simeq 8.5 \times 10^{-9}\frac{\pi^{10/3}}{a^4}(1 - n_s). \tag{32}$$

In Fig. 2, the relation $r(n_s)$ is shown for two different values of a. In the same plot, as in the weak regime, we also show the curve for standard cold inflation ($a = 0$) as well as the contours allowed by the latest Planck data. When a decreases the curve is shifted upwards, but R also decreases and eventually the condition for being in the strong dissipative regime is violated. This induces a lower bound on a. On the other hand, when a increases the curve is shifted downwards, but R also increases and the condition for being in the
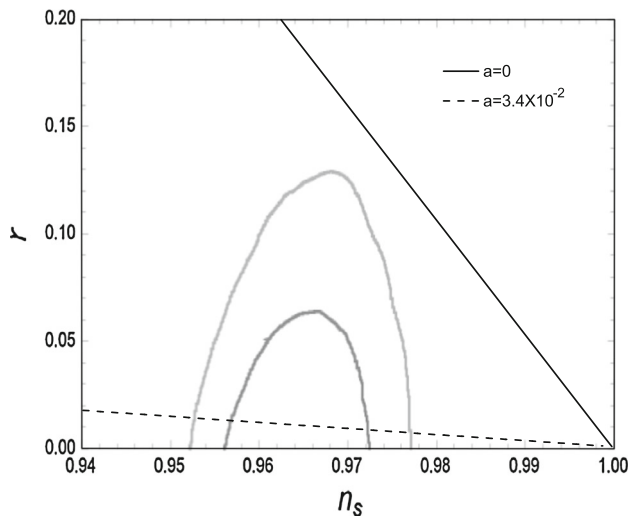

Fig. 2 Plot of the tensor-to-scalar ratio r versus the scalar spectral index n_s in the strong dissipative regime, for the quartic potential and an inflaton ratio decay $\Gamma = aT$. Here, we have considered the two-dimensional marginalized joint confidence contours for (n_s, r), at the 68 and 95 % CL, from the latest Planck data [40]. In this plot we have used two different values of the parameter a, where the value $a = 0$ corresponds to standard cold inflation

strong dissipative regime is always satisfied. This implies that there is only a lower bound for a found by the requirement of staying in the strong dissipative regime, and given by $a > 3.4 \times 10^{-2}$. Finally, Eq. (28), evaluated at 60 e-folds, gives us the constraint on λ, determined by $\lambda \sim 10^{-15}$. This value is almost the same order that obtained for λ in the standard cold inflation.

4 Conclusions

In the present work we have studied warm inflation with a quartic inflaton potential $V(\phi) = (1/4)\lambda\phi^4$ and an inflaton decay rate proportional to the temperature, namely $\Gamma = aT$. Warm inflation consists an alternative to the standard cold inflation, during which radiation is neglected and which requires two steps, a slow-roll phase followed by a reheating phase, about which very little is known. On the contrary, in warm inflation, which has the attractive feature that avoids reheating, radiation is also taken into account and it is coupled to the inflaton leading to testable predictions different from the predictions of standard inflation even in the weak dissipative regime. The model we have considered is characterized by two parameters, namely the dimensionless couplings a and λ. We have used the latest Planck data to constrain the parameters of the model, and the results we have obtained are shown in the Figs. 1 and 2 for the case of weak and strong dissipative regime, respectively. In the weak regime first, where $\Gamma \ll 3H$, the background equations look the same as in standard inflation, however, the tensor-to-scalar ratio is suppressed by the factor T/H, which must always be larger than one in warm inflation. The power spectrum constraint determines λ in terms of a, and then the tensor-to-scalar ratio as a function of the scalar index n_s changes according to a as follows: As a increases the theoretical curve is shifted downwards, and on the other hand as a decreases the theoretical curve is shifted upwards. We have obtained both an upper and a lower bound on a, since when a becomes too low the theoretical curve lies outside the contours allowed by data, and when a becomes too large the condition for the weak dissipative regime is not satisfied. In Fig. 1 we show the contours allowed by the data together with four theoretical curves, namely one for the standard inflation and for three different values of the coupling a in warm inflation, the minimum value, the maximum value and one intermediate value. In the strong dissipative regime, where $\Gamma \gg 3H$, the power spectrum does not depend on a and so the constraint determines the inflaton self-interaction coupling λ. In Fig. 2, the $r-n_s$ plot is shown and there is only a lower bound for a, obtained by the requirement of staying in the strong dissipative regime. In this regime the tensor-to-scalar ratio is suppressed by the factor T/H as in the weak regime, but also by the factor $R^{5/2}$. That is why in the strong regime the

model always predicts a very low r. By the other hand, we observe that the constraints found on the coupling λ, in both dissipative regimes, are in agreement with the value obtained in standard cold inflation using the COBE normalization. In this way, we conclude that warm inflation can rescue the quartic potential that in standard inflation is ruled out by the data.

References

1. A. Guth, Phys. Rev. D **23**, 347 (1981)
2. K. Sato, Mon. Not. R. Astron. Soc. **195**, 467 (1981)
3. A.D. Linde, Phys. Lett. B **108**, 389 (1982)
4. A.D. Linde, Phys. Lett. B **129**, 177 (1983)
5. A. Albrecht, P.J. Steinhardt, Phys. Rev. Lett. **48**, 1220 (1982)
6. A.D. Linde, Phys. Lett. B **129**, 177 (1983)
7. V.F. Mukhanov, G.V. Chibisov, JETP Lett. **33**, 532 (1981)
8. S.W. Hawking, Phys. Lett. B **115**, 295 (1982)
9. A. Guth, S.-Y. Pi, Phys. Rev. Lett. **49**, 1110 (1982)
10. A.A. Starobinsky, Phys. Lett. B **117**, 175 (1982)
11. J.M. Bardeen, P.J. Steinhardt, M.S. Turner, Phys. Rev. D **28**, 679 (1983)
12. D. Larson et al., Astrophys. J. Suppl. **192**, 16 (2011)
13. C.L. Bennett et al., Astrophys. J. Suppl. **192**, 17 (2011)
14. N. Jarosik et al., Astrophys. J. Suppl. **192**, 14 (2011)
15. G. Hinshaw et al. [WMAP Collaboration], Astrophys. J. Suppl. **208**, 19 (2013)
16. P.A.R. Ade et al. [Planck Collaboration], Astron. Astrophys. **571**, A16 (2014)
17. P.A.R. Ade et al. [Planck Collaboration], Astron. Astrophys. **571**, A22 (2014)
18. A. Pich, arXiv:0705.4264 [hep-ph]
19. P.W. Higgs, Phys. Rev. Lett. **13**, 508 (1964)
20. F. Englert, R. Brout, Phys. Rev. Lett. **13**, 321 (1964)
21. D.H. Lyth, Phys. Rev. Lett. **78**, 1861 (1997)
22. D.H. Lyth, A. Riotto, Phys. Rep. **314** (1999)
23. A. Riotto, arXiv:hep-ph/0210162
24. B.A. Bassett, S. Tsujikawa, D. Wands, Rev. Mod. Phys. **78**, 537 (2006)
25. D. Baumann, L. McAllister, arXiv:1404.2601 [hep-th]
26. A. Berera, Phys. Rev. Lett. **75**, 3218 (1995)
27. A. Berera, Phys. Rev. D **55**, 3346 (1997)
28. I.G. Moss, C. Xiong, arXiv:hep-ph/0603266
29. A. Berera, M. Gleiser, R.O. Ramos, Phys. Rev. D **58**, 123508 (1998)
30. A. Berera, R.O. Ramos, Phys. Rev. D **63**, 103509 (2001)
31. Y. Zhang, JCAP **0903**, 023 (2009)
32. M. Bastero-Gil, A. Berera, R.O. Ramos, JCAP **1107**, 030 (2011)
33. M. Bastero-Gil, A. Berera, R.O. Ramos, J.G. Rosa, JCAP **1301**, 016 (2013)
34. M. Bastero-Gil, A. Berera, R.O. Ramos, J.G. Rosa, JCAP **1410**(10), 053 (2014)
35. J. Yokoyama, A. Linde, Phys. Rev D **60**, 083509 (1999)
36. L.M.H. Hall, I.G. Moss, A. Berera, Phys. Rev. D **69**, 083525 (2004)
37. A. Berera, Phys. Rev. D **54**, 2519 (1996)
38. A. Berera, I.G. Moss, R.O. Ramos, Rep. Prog. Phys. **72**, 026901 (2009)
39. M. Bastero-Gil, A. Berera, Int. J. Mod. Phys. A **24**, 2207 (2009)
40. P.A.R. Ade et al. [Planck Collaboration], arXiv:1502.02114 [astro-ph.CO]
41. I.G. Moss, Phys. Lett. B **154**, 120 (1985)
42. A. Berera, L.Z. Fang, Phys. Rev. Lett. **74**, 1912 (1995)
43. A. Berera, Nucl. Phys B **585**, 666 (2000)
44. R. Herrera, N. Videla, M. Olivares, Eur. Phys. J. C **75**(5), 205 (2015)
45. R. Herrera, N. Videla, M. Olivares, Phys. Rev. D **90**(10), 103502 (2014)
46. R. Herrera, M. Olivares, N. Videla, Int. J. Mod. Phys. D **23**(10), 1450080 (2014)
47. A.N. Taylor, A. Berera, Phys. Rev. D **62**, 083517 (2000)
48. G. Aad et al. [ATLAS Collaboration], Phys. Lett. B **716**, 1 (2012). arXiv:1207.7214 [hep-ex]
49. S. Chatrchyan et al. [CMS Collaboration], Phys. Lett. B **716**, 30 (2012). arXiv:1207.7235 [hep-ex]
50. R. Kallosh, A. Linde, JCAP **1306**, 027 (2013). arXiv:1306.3211 [hep-th]
51. F.L. Bezrukov, A. Magnin, M. Shaposhnikov, Phys. Lett. B **675**, 88 (2009). arXiv:0812.4950 [hep-ph]
52. N. Okada, M.U. Rehman, Q. Shafi, Phys. Rev. D **82**, 043502 (2010). arXiv:1005.5161 [hep-ph]
53. S. Bartrum, M. Bastero-Gil, A. Berera, R. Cerezo, R.O. Ramos, J.G. Rosa, Phys. Lett. B **732**, 116 (2014). arXiv:1307.5868 [hep-ph]
54. M. Bastero-Gil, A. Berera, I.G. Moss, R.O. Ramos, JCAP **1405**, 004 (2014). arXiv:1401.1149 [astro-ph.CO]
55. A.R. Liddle, D.H. Lyth, (Cambridge University Press, Cambridge, 2000), p. 400